Evaluation of Railway Track Safety with a New Method for Track Quality Identification

Roberto Spinola Barbosa, Ph.D.[1]

Abstract: A new method for track inspection is developed to complement traditional geometric methods. An inertial measuring system and a specialized data treatment method is proposed to evaluate railway track safety, observed from the vehicle dynamic performance point of view. System equations for the inverse vehicle dynamic problem, augmented with the suspension torsion equation, are solved to estimate the wheels driving forces that are directly correlated with the vehicle safety traveling over an irregular track. Results of a measuring campaign on a railway wagon are used to evaluate the present system by direct positional comparison with lateral and vertical contact forces (L/V) safety ratio measured with two instrumented wheelsets (IWS) installed on the leading bogie of the wagon. Also, data collected and treated are compared with track geometry measurements. The results of quantified track safety present good agreement with those found using traditional measuring methods. This confirms the ability of the new method to detect the location of the highest potential hazard region, for optimized track maintenance purposes. The new system proves to be a promising method for track safety evaluation. **DOI: 10.1061/(ASCE)TE.1943-5436.0000855.**

Author keywords: Railway; Track; Quality; Safety.

Introduction

Railway companies always seek to operate transport systems with greater confidence and productivity. To meet this expectation, tracks should be reliable, available for use, and easy to maintain. Therefore, track quality must satisfy a set of desirable convenient properties to guarantee availability.

Different track quality indexes (TQI) have been proposed by several agencies [European Railway Agency 2011; Union Internationale des Chamins de Fer (UIC) (Nederlof and Dings 2010); Federal Railway Administration (FRA) (Stuart 2012)], but almost all are only related to geometric track issues. In fact, no safety aspect has been objectively considered. According to the Det Norske veritas (DNV) Report (European Railway Agency 2011), railway interruptions can be produced from: infrastructure failure, operational failure, and train/vehicle failure. All problems described are well quantified and mainly related to component or subsystem failure. Component failure is an event easily observable, the correlation of which is well posed. Therefore, the mentioned technique is only corrective, and some mitigation measures can be proposed.

Traditionally, railway track quality is quantified by a specialized car that measures the track's basic geometric parameters, short wavelength irregularities, and absence of complete track settlement. Usually, the inspection measures and records the variation of the track gauge, vertical and lateral alignments, and cross-level (angular variation on a track section—cant or superelevation). The values measured are compared to standardized limits. Additionally, the cross-level variation per meter (track twist) can be calculated depending on the data sample rate. Others deleterious aspects can be mentioned: lateral instability, poor wheel load equalization, vehicle overturning, longitudinal train forces, passengers' comfort (or ride quality) tailored by the vertical and lateral acceleration of the vehicle car-body, mutual vehicle/track aggression, etc. (Suarez et al. 2013).

Nevertheless, poor vehicle dynamic performance frequently occurs at a track location that does not exceed track geometry limits such as curve entry or exit or lacks track misalignments that promote vehicle yaw instability or hunting. Conversely, track geometry locations that exceed track geometry standard limits do not often cause poor vehicle performance. Poor vehicle performance may point to an area of track that needs maintenance to prevent further degradation (Ketchum and Wilson 2012).

A safety diagnosis is the ability to identify the particular region of the line where vehicle dynamic performance is poor or dangerous. To meet a security aspect, the evaluation must also consider the outcome of a lack of safety: a vehicle that effectively derails. As the track and the vehicle form a naturally mutual dependent system, the vehicle's behavior reflects its own properties and its forced movements, which are directly affected by the track geometry input, track stiffness, and train speed. This is the goal of this methodology: to include the vehicle's response in the track safety quantification.

State of the Art

Several track inspection systems or methods are still being developed. The American Federal Railway Administration has a project (Stuart 2012) to develop a system to carry out autonomous track inspections. Gullers et al. (2011) proposed a track condition analyzer (TCA) based on high-frequency vertical wheel load measurements (up to 2 kHz) performed with an instrumented wheelset (IWS) to detect mainly rail corrugations and stiff rail support. Also, the vertical wheelset acceleration (Tsunashima et al. 2014) with proper data treatment is still being researched. The European project dynamic of train (DYNOTRAIN) (Haigermoser et al. 2014) uses a multiple regression model of the vehicle dynamic behavior, within the wavelength range of 3 and 25 m, to assess track quantity. New IWS techniques are still being developed (Matsumoto et al.

[1]Professor, Dept. of Mechanical Engineering, Polytechnic School of Sao Paulo Univ. (EP-USP), Av. Prof Mello Moraes 2231, CEP 05508-970, Sao Paulo, Brazil. E-mail: spinola@usp.br

Note. This manuscript was submitted on December 19, 2014; approved on January 28, 2016; published online on June 27, 2016. Discussion period open until November 27, 2016; separate discussions must be submitted for individual papers. This paper is part of the ***Journal of Transportation Engineering***, © ASCE, ISSN 0733-947X.

2014), and others methods to estimate vehicle properties have been proposed (Pence et al. 2013). Luber et al. (2010) proposed a method for track geometry evaluation, based on a representative vehicle vertical and lateral transfer functions, to predict the vehicle response due to track geometry input.

As an acceptance process described by Wilson et al. (2011) in the state-of-the-art assessment method, a new vehicle has to demonstrate safety traveling over the track in the following conditions: low-speed flange-climbing derailment (wheel unload or body rotation resistance), vehicle dynamic response, and overturning due to overspeeding in curves. As the track's safety performance is closely affected by the track design, maintenance conditions, and effects of the local environment, it was recommended to improve measurement techniques and analysis methods. Wei et al. (2013) proposed vehicle-suspension fault detection based on acceleration sensors in the four corners of the car-body.

Calçada and Vale (2014) presents a vehicle–track dynamic-interaction one-dimension model for predicting the evolution of the vertical track profile degradation process and the attained results reveal the importance of track irregularities, vehicle speed, and vehicle characteristics on the evolution of the track profile (Hung et al. 2010). The numerical simulations demonstrate the potential of the proposed methodology to serve as a tool to forecast track settlement and estimate the dynamic response of the track along the degradation process.

Safety Fundaments

The concept of safety associated with track quality is not well described and is usually misunderstood. The track safety is the ability to promote nondangerous traffic of vehicles and trains. A vehicle transporting goods obviously depends on the track's structural integrity, efficient train operation, and the vehicle's performance to reach a minimal probability of derailment. The only way to guarantee effective track quality by focusing on safety is to objectively contemplate all these aspects including vehicle behavior.

A track's properties are mainly described by its geometric parameters such as curvature, transition curve form and length, and superelevation. Track deformation also affects the passing vehicle due its stiffness. The track usually has to be shared between passenger and freight and partial compensated (or speed-ideal) superelevations are employed. This produces a nonsymmetric wheel load distribution. Transition curve length and cant value produce a twisting variation rate, usually limited due to its influence on the vehicle suspension torsion. Finally, curve radius inhibits speed and is usually limited due to wheelset and bogie restrictions. The track irregularities are variations around the nominal geometry and may be a random or a periodic variation. As can be observed in the previous description, no safety consideration is perceived regarding the track geometry properties or roughness issue.

Regardless of the type of irregularity, the fact is that a track shape with varying geometry imposes a range of load distributions on the wheels, and their sum imposes a variation on the vehicle's kinematics. Therefore, the wheel's acting forces produce the bogie directioning and vehicle accelerations to negotiate the curves. The objective safety of the system is associated with vehicle derailment, traditionally quantified with the lateral and vertical contact forces (L/V) factor, which is well-known and widely accepted. This means that the vehicle reacts according to its transfer function to the track irregularities input. Therefore, the vehicle must be included in the evaluation process to objectively quantify the track quality from the point of view of safety.

Unsafe Types

Generally speaking, there are three types of relevant unsafe vehicle conditions. The first type is the wheel-climb derailment (Barbosa 2009). This may occur at low speed in sharp curves and is particularly related to vehicle suspension stiffness and the wheel's load-distribution condition. The second type is mainly related to large movements of a vehicle's main body. This condition can be associated with the vehicle's unsprung mass dynamic movements and directioning bogie/wheelset properties. The latter type is relative to a syntonized train speed and a particular type of track irregularities. This last one is associated the evenness of the track's wavelength, the vehicle's natural frequencies, and the specific train speed (Barbosa 2011). Although there are other types of unsafe conditions, including vehicle instability, accidents, and component failures the second type here described is mainly related to the vehicle body's low-frequency movements and small energy dissipation.

The methodology proposed here to quantify track safety is based on detecting signs of unsafe railway vehicle performance, mainly associated with the second and third types unsafe conditions when considering track evenness when traveling (Barbosa 2015). These signs are used to identify the exact location along the track and to prioritize the pertinent track geometry corrections for the most harmful irregularity to vehicle safety.

The metric adopted to identify the potential harmful location associated with the vehicle safety is the traditional L/V ratio between the wheel lateral (L) and vertical (V) contact force. The wheel forces are quantified from the measurement of the vehicle attitude and its overall dynamic behavior. This task is performed with an inverse vehicle dynamic model, fed with data acquired from the instrumented vehicle during its transit journey. The vehicle instrumentation is composed of an inertial measuring device (IMU) with nine high-resolution transducers and an inertial navigation algorithm (INS) for attitude recognition and a global positioning system (GPS) signal.

Track–Vehicle Interaction

The track irregularities are the input to the vehicle dynamics on a moving train. Track geometry variations are generally described by their circular radius, cant, and transition length. Some types of irregularities do affect the modal vehicle behavior (e.g., bounce vibration due to longwave track level or lower sway mode due to track alignment). Other track irregularities are absorbed by vehicle's suspension (e.g., short wavelength track twist). In addition, the track stiffness does affect the geometry during the vehicle passage.

The wheel–rail contact force, due to the vehicle's dynamic behavior, is a function of the roughness of the track on which the vehicle is traveling. To identify the acting contact forces that produce the vehicle's directioning movements, it is necessary to solve an inverse dynamic problem. Vehicle dynamics are described by a set of differential equations obtained from the Newton-Euler theorems applied to a model of the vehicle considered as a rigid body. This equation is valid for a fixed reference frame **N** (OXYZ) as presented in Fig. 1. For the translational movements, the following differential equations relate accelerations and external forces in an earth fixed-reference frame:

$$m^N \vec{a}_G = \sum \vec{F}^{\text{ext}} \tag{1}$$

This equation does not consider the drag and Coriolis effects from the earth rotations due to the irrelevant magnitude faced by the vehicle accelerations. The external forces are mainly due to wheel contact forces and gravitational effects as shown in Fig. 1.

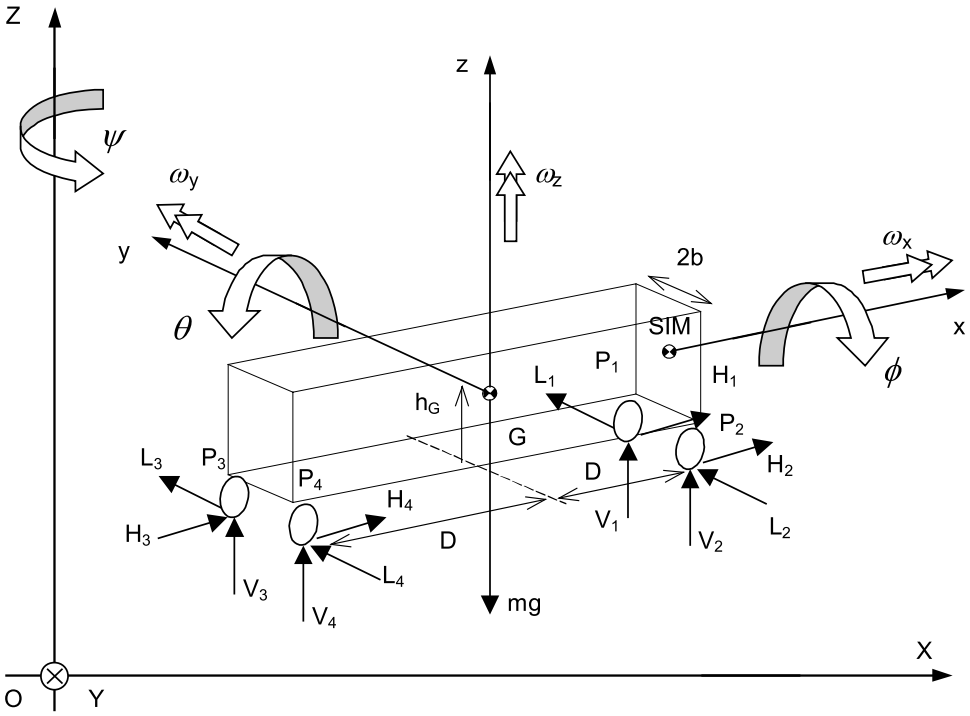

Fig. 1. Body attitude and forces distribution on the vehicle

$$m^N\vec{a}_G = \sum \vec{F}_{\text{wheels}} - m^N\vec{g} \tag{2}$$

The equation can also be expressed in the body reference frame (Gxyz) using a rotational transformation matrix $\boldsymbol{T}$, composed of the three Euler angles (roll ϕ, pitch θ, and yaw ψ) as identified in Fig. 1, from which the accelerations are to be measured and the forces computed

$$mT_N^B({}^N\vec{a}_G + {}^N\vec{g}) = T_N^B \sum \vec{F}_{\text{wheels}} \tag{3}$$

When the measuring system is fixed at a particular point P, not coincident with the vehicle center of gravity $\boldsymbol{G}$, the measured acceleration must be projected according to the field acceleration equation, to be used by the Newton equation

$$\vec{a}_G = \vec{a}_P + \dot{\vec{\omega}} \wedge (G-P) + \vec{\omega} \wedge [\vec{\omega} \wedge (G-P)] \tag{4}$$

where the angular velocity $\vec{\Omega} = \dot{\phi}\,\vec{i} + \dot{\theta}\,\vec{j}' + \dot{\psi}\,\vec{K}$, composed of roll rate $\dot{\phi}$, pitch rate $\dot{\theta}$, and yaw rate $\dot{\psi}$. For the rotational movements described in a moving reference frame attached to the vehicle, the following differential equations relate angular accelerations $\dot{\omega}$ and body angular velocity $\omega_B = [\,\omega_x \quad \omega_y \quad \omega_z\,]^T$ and external moments with respect to the same pole:

$$[J]_G\{\dot{\omega}\} + [\omega_B] \wedge [J]_G\{\omega_B\} = \{M_G^{\text{ext}}\} \tag{5}$$

The body external contact forces due to each wheel (H_i, L_i, and V_i) are shown in Fig. 1. The body external moments (M_G) due to the wheel forces are obtained from the car-body dimensions as shown in Fig. 1. To work out the contact forces by solving the system equation, it is necessary to know the vehicle body's accelerations, as stated in Eq. (1). Additionally, it is also necessary to measure the angular velocity and estimate the angular acceleration, which are needed to solve Eq. (2). Finally, the body's angular attitude must be identified to solve torsion Eq. (6).

The system has six equations and 12 contact-force unknowns. Disregarding the longitudinal effects, one equation is removed and four longitudinal contact forces are ignored (no acceleration or breaking effects). Due to the system being hyperstatic, the contact lateral forces in each wheelset are summed. To solve the system with five equations and six unknowns, an additional suspension torsion equation is disclosed to access each vertical force relationship, completing the system.

The vehicle longitudinal torsion due to track twist affects mainly the vertical wheel load distribution. Considering the car structure as a rigid body, the track twist deflects the suspension unloading the diagonal wheels. This effect depends on the vehicle suspension stiffness, length and width of the vehicle, and magnitude and wavelength of track twist.

Namely, the expression for the vertical load variation as a function of the track's angular twist per meter (δ) is related to body geometry proportion ($D/2b$) and suspension torsional stiffness (k_ϕ) stated as

$$\Delta V = -k_\phi \frac{D}{2b}\delta \tag{6}$$

To estimate the track twist from the overall vehicle inclination, a special filter is used to recover the local track superelevation (α). However, the IMU coupled to the body measures the absolute vehicle roll angle in reference to the earth plane (ϕ). The total or earth referenced body angle, as shown in Fig. 2, is composed by the track cant angle (α) added to the relative vehicle roll angle (β) due to suspension movements and inertial mass center height (h_G)

$$\phi = \alpha + \beta \tag{7}$$

The track cant angle (α) can be measured with an additional IMU installed on the wheelset. If this value is not available, another identification method is necessary. Disregarding any small vehicle suspension roll, the twist variation can be obtained from

J. Transp. Eng., 2016, 142(11): 04016053

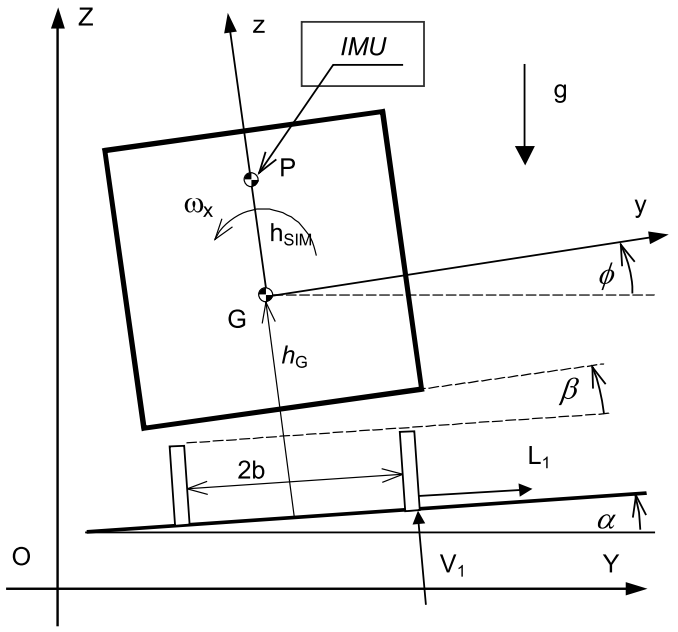

Fig. 2. Track and vehicle roll angles

$$\delta = \frac{d\alpha}{dS} \tag{8}$$

To identify the angles and attitude, the inertial navigation algorithm (INS) based on an extended Kalman filter is used as a multivariable estimator. With all this information, it is possible to solve the vehicle inverse dynamic equations to evaluate the driving contact forces and calculate the traditional safety ratio force L/V. Only for facility, a safety index (SI) for track safety quantification, calculated as the difference between the maximum L/V limit and the module of the measured L/V value for each wheel (Barbosa 2004), is used

$$SI = \left|\frac{L}{V}\right|_{\text{Limit}} - \left|\frac{L_i}{V_i}\right|_{\text{measured}} \tag{9}$$

To solve the inverse identification problem, the model of the system has to be known, have a unique existing solution, and continuously have data on the system available. Therefore, the requirements for the solution of the inverse problem are available using a complete measuring system, continuously monitoring vehicle body movement, and its attitude's dynamic behavior.

Measuring System and Data Treatment

The measuring system consists of an inertial measurement unit fixed on the vehicle, a GPS (uBlox, Switzerland) and a computer (Dell, Texas) for command actions, data acquisition and storage media. The inertial measurement unit (Honeywell, Morristown, New Jersey) is a micro-electro-mechanical system (MEMS) that measures the body movement. It utilizes a set of triorthogonal accelerometers to measure the vehicle accelerations ${}^{B}\vec{a}_G$ and an angular speed device to measure attitude variation ${}^{B}\vec{\omega}$. Additionally, a triorthogonal magnetometer set and a precision barometer measures the orientation ${}^{B}\vec{m}$ based on the earth's magnetic field and the relative level. A GPS identifies the vehicle speed and position expressed in the geographic-referenced latitude and longitude coordinate system. All this information is antialiasing filtered, digitalized, and recorded in the on-board control computer to identify the vehicle's three-dimensional movements.

To recover the complete vehicle attitude to calculate the SI index, an algorithm based on attitude heading reference system (AHRS) is used to treat rough data from the sensor and identify vehicle attitude. Vehicle accelerations and angular attitude are the main information to recover from the accelerometers, rate-gyros, and magnetometers information. To this end, a local-level frame identification algorithm must be involved for the vehicle's angular attitude recognition. An integrated navigation system on terrestrial movement methodology should combine the measured state data, with independent redundant data in a Kalman filter algorithm to provide a long-term stable solution. The strapdown inertial recovery (SIR) system identifies the external loads by solving the vehicle's dynamic equations.

The vehicle attitude relative to an inertial reference frame $\boldsymbol{N}$, is described by three Euler angles denoting vehicle roll angle ϕ, elevation angle θ, and heading angle ψ as shown in Fig. 1. The absolute position of a point in the vehicle is described by the vector ${}^{N}\vec{r}$ expressed in the inertial reference frame $\boldsymbol{N}$ and its time rate of change as

$${}^{N}\vec{r} = T_B^{NB}\vec{r} \quad \text{and} \quad {}^{N}\dot{\vec{r}} = T_B^{NB}\dot{\vec{r}} + \dot{T}_B^{NB}\vec{r} \tag{10}$$

where the superscript N over the vector = the fixed reference frame and the superscript B = the body fix moving reference frame; T_B^N = direction cosine matrix (DCM) formed with the three Euler rotation angles, which leads to the transformation matrix in terms of the three successive sequential body rotations [Sequence 3-2-1, according to NASA Standard (Baruh 1999)]

$$T_B^N = \begin{bmatrix} c\theta\, c\psi & c\theta\, s\psi & -s\theta \\ -c\theta\, s\psi + s\phi\, s\theta\, c\psi & c\theta\, c\psi + s\phi\, s\theta\, s\psi & s\phi\, c\theta \\ s\phi\, s\psi + c\phi\, s\theta\, c\psi & -s\phi\, c\psi + c\phi\, s\theta\, s\psi & c\phi\, c\theta \end{bmatrix} \tag{11}$$

where prefixes s and c = for sine and cosine for the respective angle.

The velocity vector ${}^{N}\vec{V}$ expressed in the inertial fixed frame $\boldsymbol{N}$ is defined in terms of position ${}^{B}\vec{r}$ expressed in rotating body fix reference $\boldsymbol{B}$, as

$${}^{N}\vec{V} = T_B^N\ {}^{B}\dot{\vec{r}} \text{ and its time derivative as } {}^{N}\vec{a} = \dot{T}_B^N\ {}^{B}\dot{\vec{r}} + T_B^N\ {}^{B}\ddot{\vec{r}} \tag{12}$$

The relation between the body angular velocities ω_B (roll rate, pitch rate, and yaw rate) and the vehicle attitude rate Ω_N (rate in bank, attitude, and heading) is described by Baruh (1999)

$$\begin{Bmatrix} \omega_x \\ \omega_y \\ \omega_z \end{Bmatrix} = \begin{bmatrix} 1 & 0 & -s\theta \\ 0 & c\phi & s\phi\, c\theta \\ 0 & -s\phi & c\phi\, c\theta \end{bmatrix} \begin{Bmatrix} \dot{\phi} \\ \dot{\theta} \\ \dot{\psi} \end{Bmatrix} \tag{13}$$

and the time rate of change of the transformation matrix $\dot{T}_N^B$ is

$$\dot{T}_B^N = T_B^N\, \omega_B \quad \text{where } \omega_B = \begin{bmatrix} 0 & -\omega_z & \omega_y \\ \omega_z & 0 & -\omega_x \\ -\omega_y & \omega_x & 0 \end{bmatrix} \tag{14}$$

where ω_i = the three angular speeds components described in the skew symmetric rotating matrix expressed on the body reference frame.

The problem of attitude determination involves determining the transformation matrix that maps the information sensed on-board with model transformation to the geographic frame magnetic and

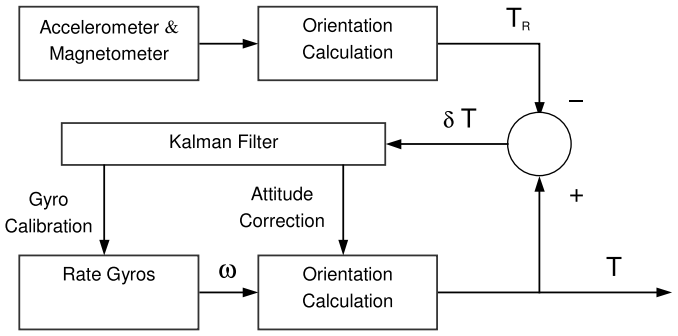

Fig. 3. Block diagram

gravity field components (Kuga and Carrara 2013). For the body-referenced magnetic sensor to match the local geographic-referenced magnetic field, and for the body-referenced accelerometer sensor to match the local geographic-referenced acceleration, then

$$^{N}\vec{m} = T_B^{NB}\vec{m} \quad \text{and} \quad ^{N}\vec{a}_G = T_B^{NB}\vec{a}_G \tag{15}$$

Assuming these two vectors are not parallel, a third orthogonal vector can be produced by the cross product. The matrix formed using these three vectors as columns (superscript T over the vector = transposed vector) can be associated with

$$[^{N}\vec{m}^T \quad ^{N}\vec{a}^T \quad (^{N}\vec{m} \wedge ^{N}\vec{a})^T] = T_B^N\,[^{B}\vec{m}^T \quad ^{B}\vec{a}^T \quad (^{B}\vec{m} \wedge ^{B}\vec{a})^T] \tag{16}$$

The matrix on the left-hand side is composed by known geographic-referenced information. The matrix on the right-hand side is composed of sensed information. Therefore, the unknown DCM orthogonal matrix can be obtained from

$$T_B^N = [^{B}\vec{m}^T \quad ^{B}\vec{a}^T \quad (^{B}\vec{m} \wedge ^{B}\vec{a})^T]^T[^{N}\vec{m}^T \quad ^{N}\vec{a}^T \quad (^{N}\vec{m} \wedge ^{N}\vec{a})^T]$$
$$\text{and} \quad T_N^B = (T_B^N)^T \tag{17}$$

A more-refined estimation for the DCM matrix to identify body attitude is obtained using a Kalman filter technique (Marins et al. 2001). Typical integration accumulated drift errors, such as heading vehicle attitude, are to be corrected with multiple cross-sensor information. With the accelerometers and the magnetometer, a level frame is to be determined. Based on this error difference, an extended Kalman filter algorithm corrects and stabilizes the rate-gyros' orientation calculations as shown in Fig. 3. Complementary GPS data allows estimating the vehicle speed, alignment, and curvature of the trajectory (Anderson and Bevly 2010).

The angular description can be in the Euler angles or Quaternion form, depending on the need to solve the singular problems due to angular quantification. With the accelerations, angular rate, and attitude angles, the vehicle's guiding force is calculated with the aid of a strapdown inertial recovery (SIR) algorithm that allows determination of the vehicle's L/V safety index. Data were previously filtered with a low-pass 15 Hz FIR filter.

Validation Process

The validation process of the proposed system was based on the comparison of the safety index (SI) calculated with the SIR algorithm, with measured bogie L/V wheel forces ratio acquired with two IWS.

The L/V wheel force ratio was measured with two Swedish instrumented wheel sets (IWS) (Interfleet, Sweden) installed on the leading bogie of the wagon. For compatible direct comparison with SIR results, the bogie L/V values were calculated from the sum of the lateral load of each wheel divided by the sum of the vertical measured loads. Speed and position of the train along the track were acquired with a GPS.

The track geometry and irregularities, measured with a specialized measuring car, are employed to complement the evaluation. Track geometry has an indirect correlation with safety but contributes to it and is also used in the comparison process. The measuring car (Plasser EM-100, Plasser & Theurer, Austria) was used to measure the variation of the track gauge, vertical and lateral rail alignments (left and right), and track section cant. Additionally, it identifies track curvature and track twist.

Test Campaign

A special test train was prepared to travel along a selected track section (Fig. 4). The train was formed with two locomotives (one at each end), four iron-ore 120-t loaded wagons (Fig. 5),

Fig. 4. Train formation (image by the author)

Fig. 5. 120-t iron ore wagon (image by the author)

Fig. 6. Instrumented wheelsets and measuring system (image by the author)

and two laboratory cars. The SIR system was installed underneath the first wagon as can be observed in Fig. 6. The two IWS are installed in the leading bogie of this wagon. The selected 25-km track section goes from 35 to 10 km (in the east sense) of the Carajas railway located in the northern region of Brazil. There are some curves and a bridge over a sea firth. This railway is 1.6-m gauge with almost 900 km connecting the Carajas Mine to the Sao Luiz port. The typical iron-ore wagon is a 120-t gondola *GDT*, with 0.1778×0.2794 m (7×11 in.) ride-control bogies.

Several tests were performed in this track section in the eastbound direction (traveling from mine to port, which is typical for the loaded wagon) at a constant speed and returning in the westbound direction at maximum authorized speed.

General Results

Several tests were conducted at controlled speeds (30, 50, 60, 70, and 75 km/h) in the eastbound direction (mine to port). The test

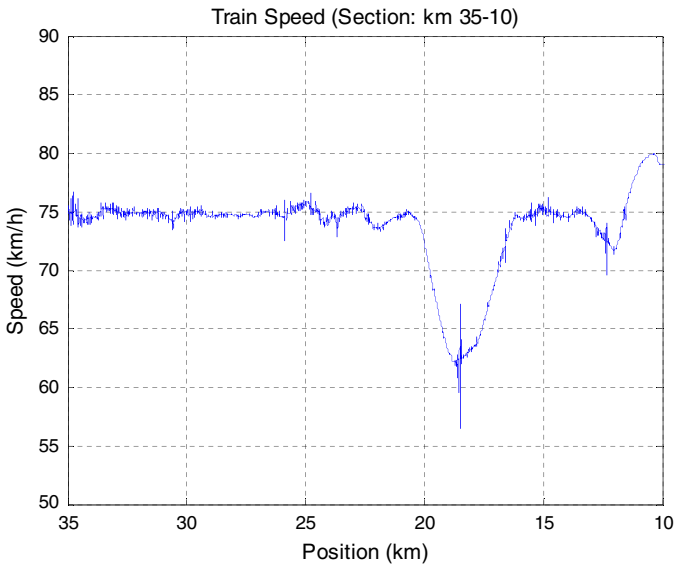

Fig. 7. Train speed

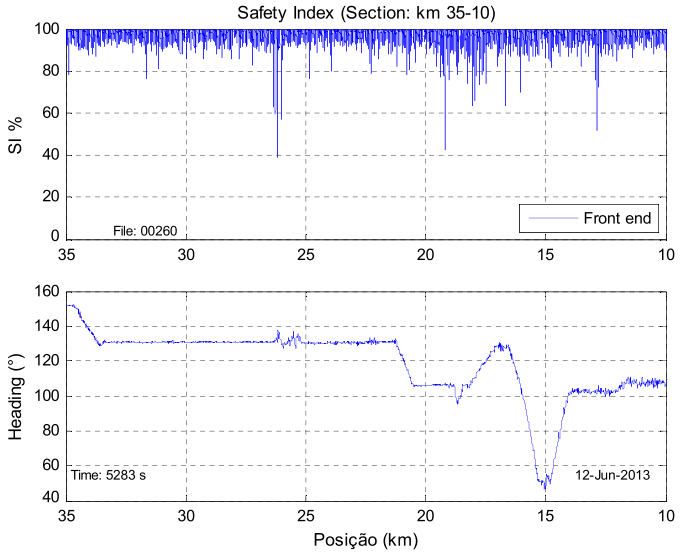

Fig. 8. Safety index ($35 + 000$ until $10 + 000$ km)

at 75 km/h was selected for a closer analysis. The train speed was expected to be constant but due to restrictions near a bridge, the real speed varied around programmed values and its time history is presented in Fig. 7. The track SI values determined in function of kilometric position are presented in the upper graph of Fig. 8. The lower graph in this figure shows the heading of the wagon.

The track geometry of this section, as measured with the EM-100 measuring car, is presented in Fig. 9. The upper graph shows the track cant along the kilometric position and the lower graph the track curvature. The wagon heading (lower graph in Fig. 8) is compatible and synchronized with the track curvature (lower graph in Fig. 9) measured with EM-100 car.

The L/V for the leading bogie, calculated from measured values of the two wheelsets, is presented in Fig. 10.

Particularly three track subsections are analyzed in detail. Results are presented as follow.

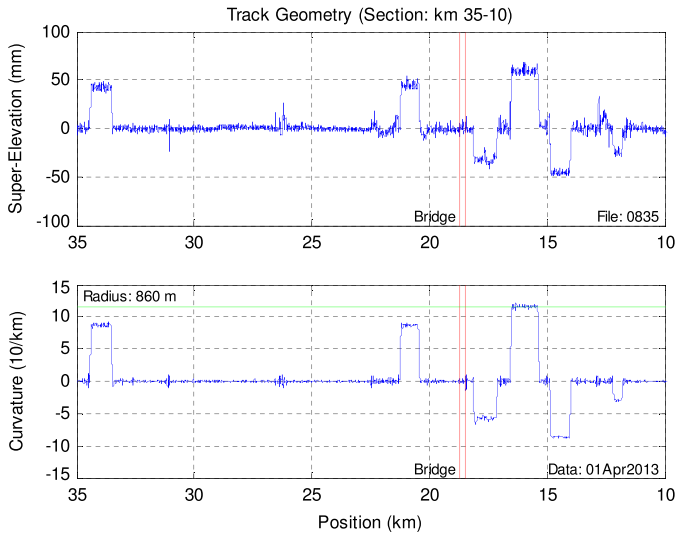

Fig. 9. Track-measured geometry (EM-100 measuring car)

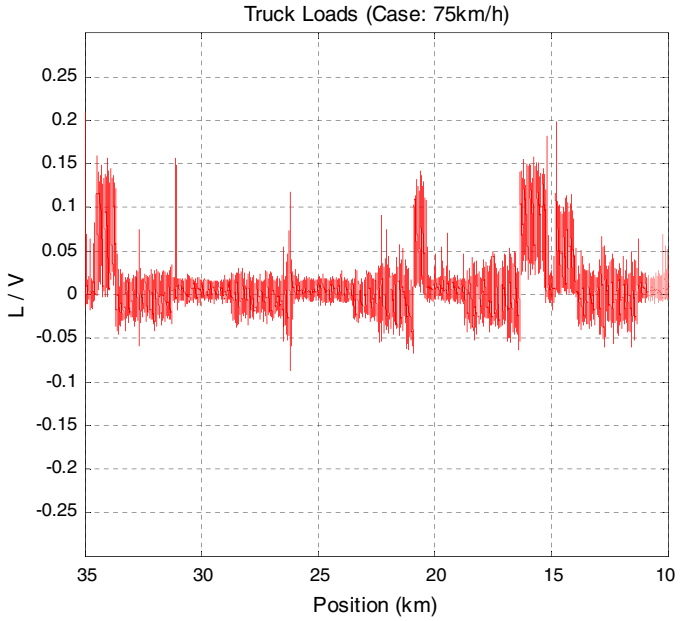

Fig. 10. Leading bogie L/V results

Subsection between 13.5 and 12 km

The subsection between kilometers $13+500$ and $12+000$ is a tangent segment of track as described by the wagon heading presented in the lower graph of Fig. 11. A SI of at least 50% is identified at $12+800$ km, as shown in the upper graph of Fig. 11.

The track geometry measurements detect a superelevation point of 30 mm at $12+800$ km, as shown in Fig. 12. In this region, the measured track twist variation is approximately -25 mm (Fig. 13). The leveling reaches -28 mm maximum, as shown in Fig. 14. The track alignment deviation of ± 8 mm can also be verified. The track gauge-widening reaches 10 mm, as shown in Fig. 13. Therefore the poor track geometry is correspondently identified with the SIR system. The safety in this track subsection is confirmed with the L/V measured with the instrumented wheelsets of ± 0.06, as shown in Fig. 15.

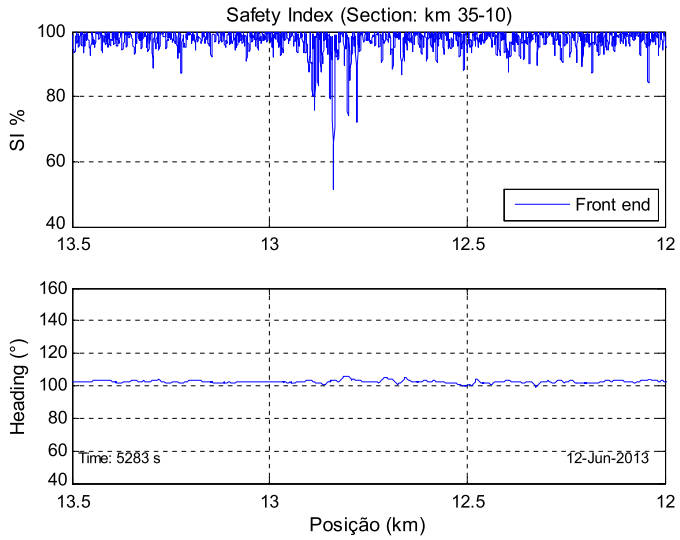

Fig. 11. Safety index and heading (13.5–12 km)

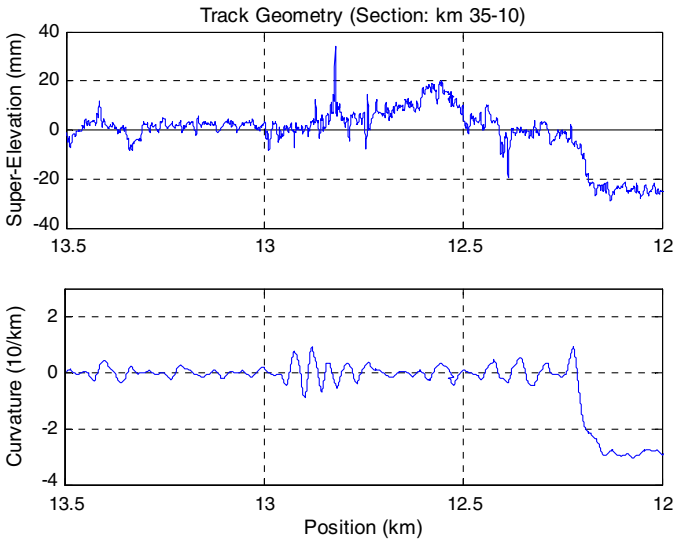

Fig. 12. Track superelevation and curvature (13.5–12 km)

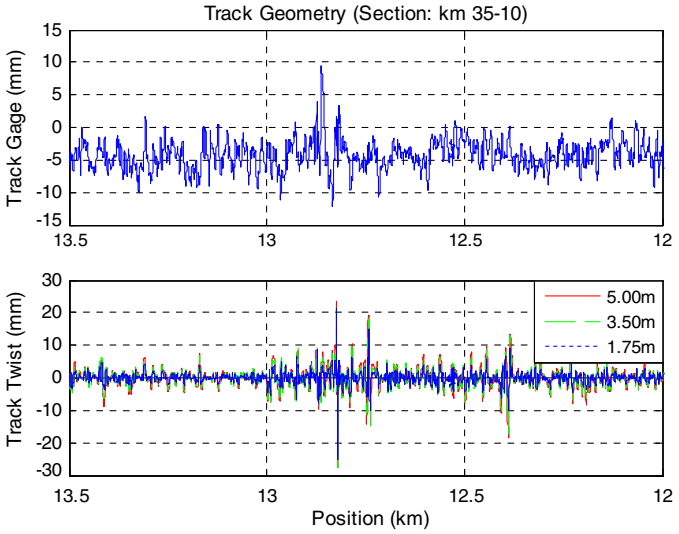

Fig. 13. Track gauge and twist (13.5–12 km)

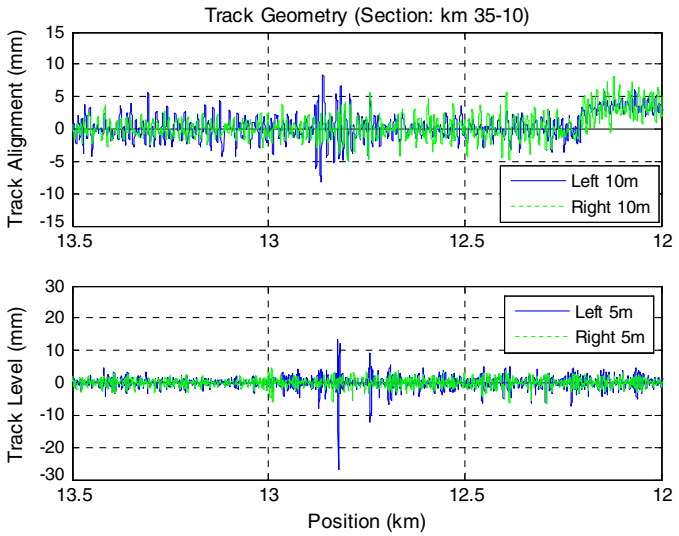

Fig. 14. Track alignment and level (13.5–12 km)

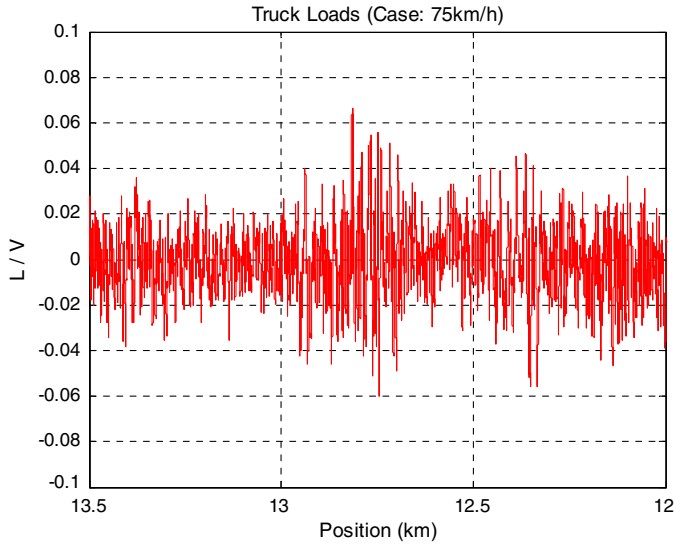

Fig. 15. Measured L/V for the front bogie (IWS) (13.5–12 km)

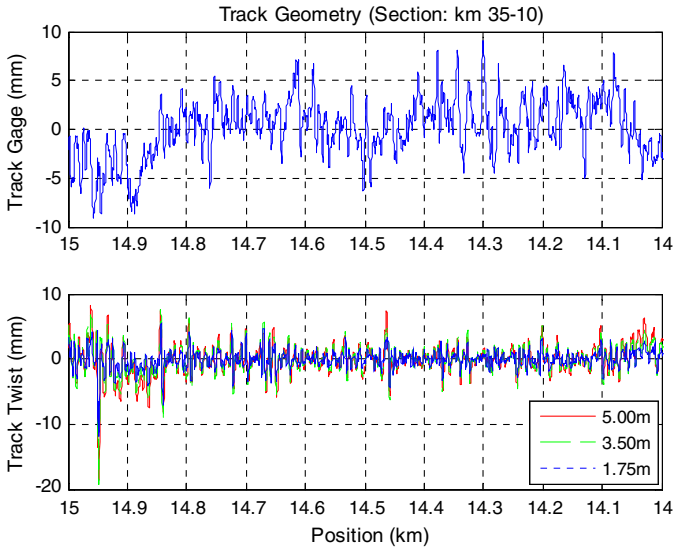

Fig. 17. Track gauge and twist (from 15 to 14 km)

Subsection between 15 and 14 km

The subsection between 15 + 000 and 14 + 000 km has been also analyzed in detail. In this section, there is a curve with a 1,150 m radius that starts at 14 + 900 km, considering the eastbound traffic. It is observed that the SI had a value of at least 80% just after the transition curve, as shown in Fig. 16.

Although the track geometry does not present any significant variations (Figs. 17 and 18) in this region, the L/V measured with instrumented wheelsets for the leading bogie shows a relevant peak of 0.2, as shown in Fig. 19, confirming the correct SIR identification.

Subsection from 31 + 500 *to* 30 + 500 km

The subsection between 31 + 500 and 30 + 500 km is a tangent segment of the track. At 31 + 100 km, an SI of at least 80% was identified, as shown in Fig. 20. A sudden change is noticed in the superelevation value, to 23 mm at 31 + 080 km, as shown

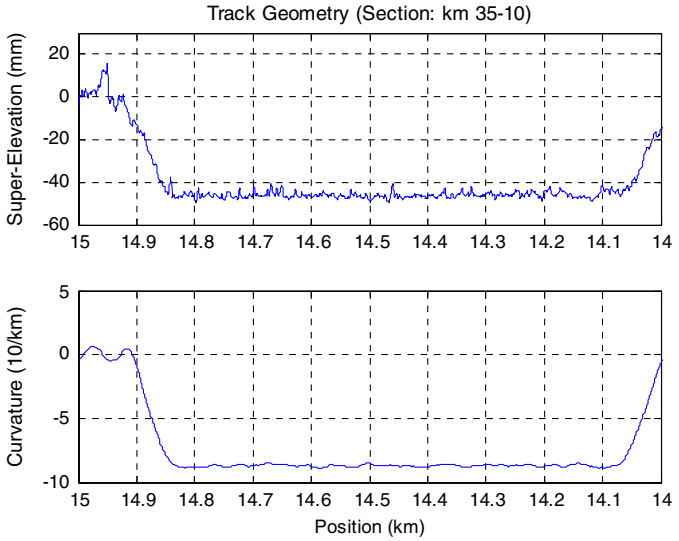

Fig. 18. Track superelevation and curvature (from 15 to 14 km)

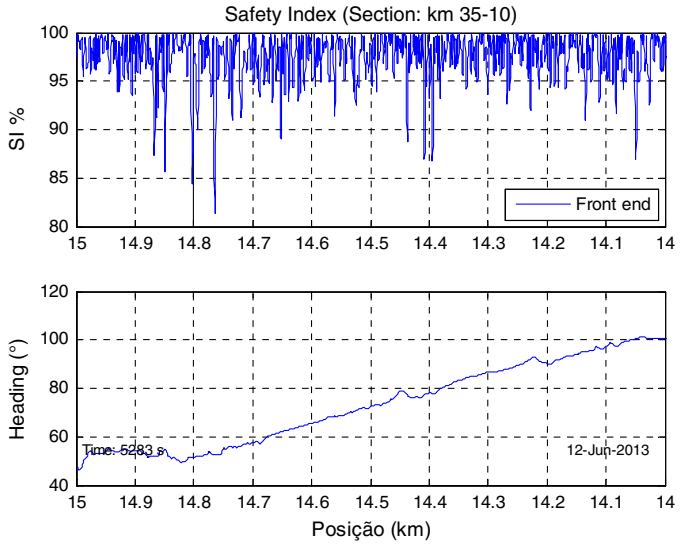

Fig. 16. Safety index (from 15 to 14 km)

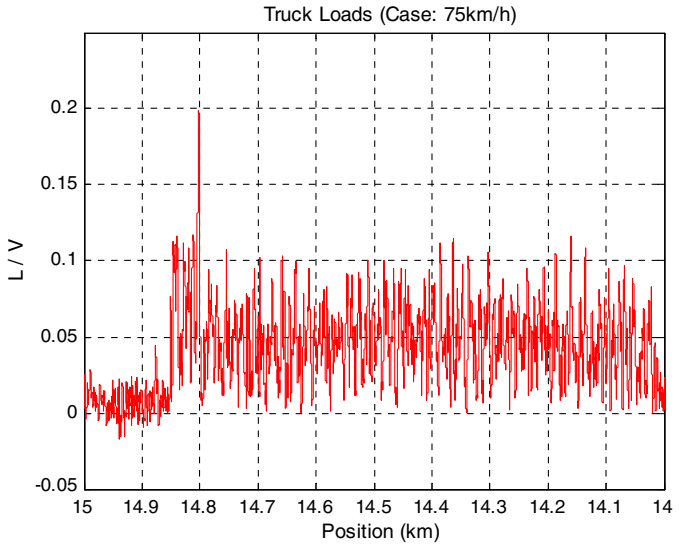

Fig. 19. Leading bogie L/V (from 15 to 14 km)

Fig. 20. Safety index (31 + 500 to 30 + 500 km)

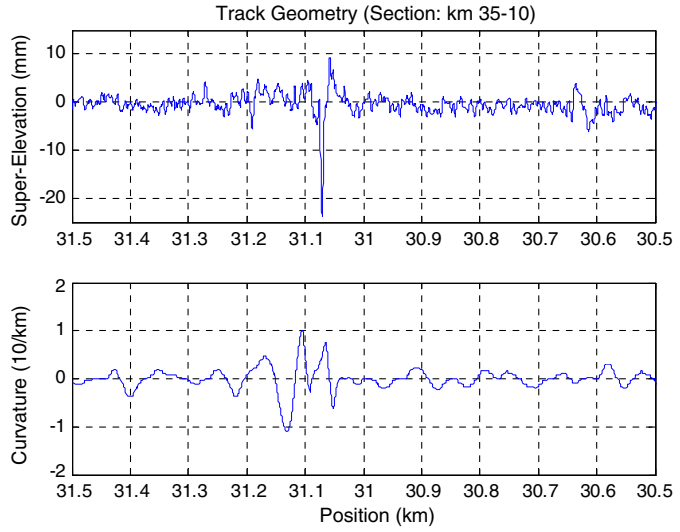

Fig. 21. Track superelevation and curvature (31.5–30.5 km)

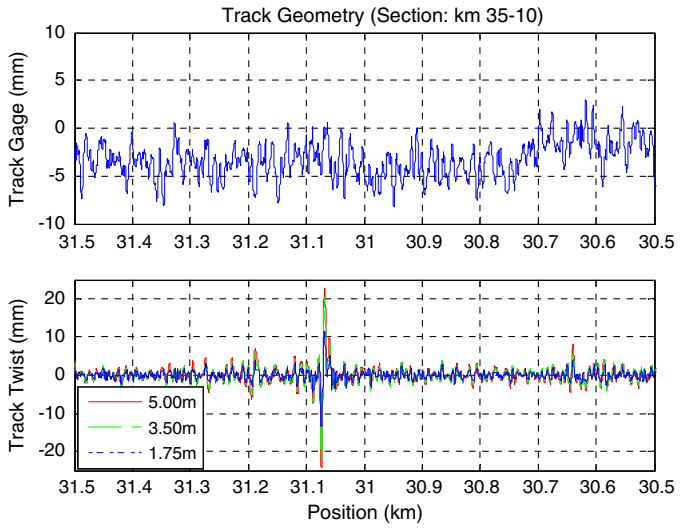

Fig. 22. Track gauge and twist (31.5–30.5 km)

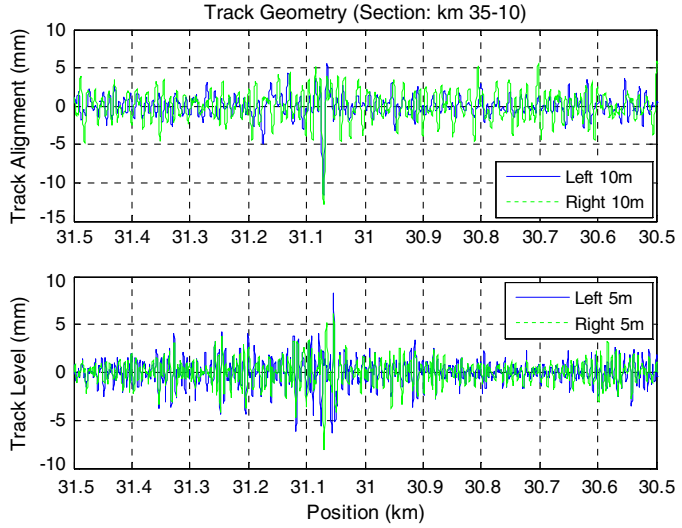

Fig. 23. Track alignment and level (31.5–30.5 km)

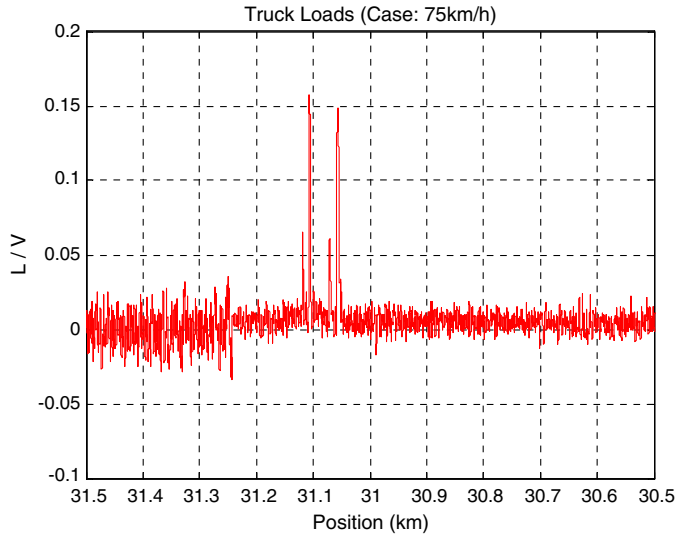

Fig. 24. Leading bogie L/V (31.5–30.5 km)

in Fig. 21. At this point, the track twist reached ±23 mm (Fig. 22). There is also a sudden change in the track alignment, shown in Fig. 23. Therefore, the poor geometry is correspondently identified using the SIR system. Safety at this point is confirmed with the L/V measured with the instrumented wheelsets of 0.15, as shown in Fig. 24.

Discussion

Obviously, the magnitudes of the results are related to the speed of the train during the journey. The operating speed varied depending on the driver style, train load, weather conditions, and any speed restrictions existing on the track. However, at different speeds, the magnitude of forced movements will change, altering the magnitude of the identified L/V values but keeping the position of the harmful location. Even the natural movements, induced by periodic irregularities, change due to the suspension's damping factor, but the position remains. The process is deterministic and depends on the initial conditions and speed. Therefore, system

repeatability may be spread due to initial conditions and speed variability.

Even a wagon with chronic lateral instability will correctly identify the undesirable type of track irregularity, according to its own point of view. A spectral analysis can easily identify this wagon feature due to its periodic characteristic behavior.

This method also takes into account the effects of nonstationary train longitudinal coupler forces, albeit unnecessarily from the point of view of track quality. This action does affect the wheel load distribution and safety as a consequence, particularly in curves where its projection affects the lateral acceleration and the angular yaw body acceleration. Therefore, this *jerk* phenomenon is characterized by the body angular accelerations accordingly recovered.

This quantification method complements other existing geometric tools. The possibility of evaluating similar vehicles across various load conditions or distinct vehicle fleets is easily performed simply by changing the installation of the measuring device. The data measured can also be used to evaluate passenger comfort using the vertical and lateral accelerometers' signals in accordance with the comfort standard [ISO 2631 (ISO 2001)] or even the vehicle modal quantification. Differently from other systems that use only statistical information from a few sensors, the system presented herein is MISO, which takes into account the vehicle's complete multisignal input and delivers a single output index directly correlated to the track's safety condition.

Conclusion

An inertial measuring system and a specialized data treatment method to perform the railway track quality and safety quantification as observed from the vehicle performance point of view is presented. Using a strapdown inertial recovery (SIR) method, the system measures the vehicle's dynamic movements and attitude during its transit along an irregular track. The values measured are used in an attitude heading reference system (AHRS) algorithm with an extended Kalman filter to identify the full vehicle attitude, including angular positions and accelerations. The vehicle system equations for the inverse dynamic problem, augmented by suspension torsion equation, are solved to directly calculate the wheels' driving forces. The safety L/V contact force ratio at low frequency is identified. A safety index (SI), which is directly correlated with vehicle safety, is determined based on the railway's L/V safety limits. Values obtained are used to qualify the most harmful track locations.

A field test program was conducted in a special train traveling at controlled speed. The system was installed on a loaded iron ore wagon and the train ran on a selected track section at various speeds. The track SI quantification was directly compared with measures of the IWS. Results show good agreement between both systems. Additionally, the results are also compared with the measured geometry of the local track and variations are confirmed with the new system results. The GPS signal simultaneously captures the train speed and the exact georeferenced location of the highest potential hazard region for track maintenance purposes.

Due to its simplicity and low cost, the new system can be easily installed in any vehicle and operate with any load condition and at variable traveling speeds, without the traditional traffic disturbance. The system can be applied to any specific vehicle fleet, traveling on any track section, at the usual operational speed, and detect the most harmful track location to complement geometric measuring methods. The analyses can also be focused to compute different priority criteria (passenger comfort, minimal dynamic vertical load applied to the track, instantaneous safety indicator, etc.) according to user interests. Better classification of the most harmful track locations allows prioritizing the track intervention strategy. The complementary combination of new and traditional monitoring track-inspection techniques can help to better understand asset behavior and produce effective investment efficiency in railway track maintenance, and is thus a promising technique.

Acknowledgments

The author would like to thank the Mechanical Department of the Engineering School of the University of Sao Paulo (EP-USP) for the support to this research, engineer Guilherme Fabiano dos Santos and VALE S.A., which organized and made available the railway resources for the validation tests.

References

Anderson, R., and Bevly, D. M. (2010). "Using GPS with a model-based estimator to estimate critical vehicle state." *Veh. Syst. Dyn.*, 48(12), 1413–1438.

Barbosa, R. S. (2004). "A 3D contact force safety criterion for flange climb derailment of a railway wheel." *J. Veh. Syst. Dyn.*, 42(5), 289–300.

Barbosa, R. S. (2009). "Safety of a railway wheelset-derailment simulation with increasing lateral force." *Veh. Syst. Dyn.*, 47(12), 1493–1510.

Barbosa, R. S. (2011). "Vehicle dynamic response due to pavement roughness." *J. Braz. Soc. Mech. Sci. Eng.*, 33(3), 302–307.

Barbosa, R. S. (2015). "New method for railway track quality identification through the safety dynamic performance of instrumented railway vehicle." *J. Braz. Soc. Mech. Sci. Eng.*, 10.1007/s40430-015-0471-9, 1–11.

Baruh, H. (1999). *Analytical dynamics*, McGraw-Hill, 419.

Calçada, R., and Vale, C. (2014). "A dynamic vehicle-track interaction model for predicting the track degradation process." *J. Infrastruct. Syst.*, 10.1061/(ASCE)IS.1943-555X.0000190, 04014016.

European Railway Agency. (2011). "Assessment of freight train derailment risk reduction measures: B1–Derailment risk models. Det Norske Veritas–DNV: Report for European Railway Agency." *Rep. No. BA000777/06(2)*, Valenciennes, France.

Gullers, P., Dreik, P., Nielsen, J. C. O., Ekberg, A., and Andersson, L. (2011). "Track condition analyser: Identification of rail rolling surface defects, likely to generate fatigue damage in wheels, using instrumented wheelset measurements." *Proc. Inst. Mech. Eng. F J. Rail Rapid Transit.*, 225(F1), 1–13.

Haigermoser, A., et al. (2014). "Describing and assessing track geometry quality." *Veh. Syst. Dyn.*, 52(Suppl. 1), 189–206.

Hung, C., et al. (2010). "Study on detection of the early signs of derailment for railway vehicles." *Veh. Syst. Dyn.: Int. J. Veh. Mech. Mobility*, 48(Suppl. 1), 451–466.

ISO. (2001). "Mechanical vibration and shock—Evaluation of human exposure to whole-body vibration. Part 4: Guidelines for the evaluation of the effects of vibration and rotational motion on passenger and crew comfort in fixed-guideway transport systems." *ISO 2631*, Geneva.

Ketchum, C. D., and Wilson, N. (2012). "Performance-based track geometry—PBTG. Phase: 1. Transit cooperative research program." *Document 52*, Transportation Technology Center, 89.

Kuga, H. K., and Carrara, V. (2013). "Attitude determination with magnetometers and accelerometers to use in satellite simulator." Hindawi Publishing Corporation, Cairo, Egypt, 1–6.

Luber, B., Haigermoser, A., and Grabner, G. (2010). "Track geometry evaluation method based on vehicle response prediction." *Veh. Syst. Dyn.: Int. J. Veh. Mech. Mobility*, 48(Suppl. 1), 157–173.

Marins, J. L., Yun, X., Bachmann, E. R., McGhee, R. B., and Zyda, M. J. (2001). "An extended Kalman filter for quaternion-based orientation estimation using MARG sensors." *Proc., 2001 Int. Conf. on Intelligent Robots and Systems*, IEEE, 2003–2011.

Matsumoto, A., et al. (2014). "Actual states of wheel/rail contact forces and friction on sharp curves—Continuous monitoring from in-service trains and numerical simulations." *Wear*, 314(1–2), 189–197.
Nederlof, C., and Dings, P. (2010). "Monitoring track condition to improve asset management." Union International Chamin de Fer–UIC, Paris.
Pence, B., et al. (2013). "Vehicle sprung mass estimation for rough terrain." *Int. J. Veh. Des.*, 61(1/2/3/4), 3–26.
Stuart, C. (2012). "Autonomous track geometry measurement system (ATGMS). Reseach and development review." Federal Railway Administration (FRA), Dept. of Transportation (DOT), Washington, DC, 22.
Suarez, B., Felez, J., Lozano, J. A., and Rodriguez, P. (2013). "Influence of the track quality and of the properties of the wheel—Rail rolling contact on vehicle dynamics." *Veh. Syst. Dyn.*, 51(2), 301–320.
Tsunashima, H., Naganuma, Y., and Kobayashi, T. (2014). "Track geometry estimation from car-body vibration." *Veh. Syst. Dyn.*, 52(1), 207–219.
Wei, X., Jia, L., and Liu, H. (2013). "A comparative study on fault detection methods of rail vehicle suspension systems based on acceleration measurements." *Veh. Syst. Dyn.*, 51(5), 700–720.
Wilson, N., et al. (2011). "Assessment of safety against derailment using simulations and vehicle acceptance tests: A worldwide comparison of state-of-the-art assessment methods." *Veh. Syst. Dyn.*, 49(7), 1113–1157.